

# X-band ESEEM spectroscopy of $^{15}\text{N}$ substituted native and inhibitor-bound superoxide dismutase

## Hyperfine couplings with remote nitrogen of histidine ligands

Sergei Dikanov<sup>a,b</sup>, Isabella Felli<sup>c</sup>, Maria-Silvia Viezzoli<sup>c</sup>, Andrei Spoyalov<sup>b</sup>, Jürgen Hüttermann<sup>a,\*</sup>

<sup>a</sup>Fachrichtung Biophysik und Physikalische Grundlagen der Medizin, Universität des Saarlandes, Klinikum Bau 76, 66421 Homburg (Saar), Germany

<sup>b</sup>Institute of Chemical Kinetics and Combustion, Russian Academy of Sciences, Novosibirsk 630090, Russian Federation

<sup>c</sup>Department of Chemistry, University of Florence, Via G. Capponi 7, 50121 Florence, Italy

Received 27 November 1993; revised version received 11 April 1994

### Abstract

The hyperfine couplings of the remote nitrogens of histidine ligands are determined for the first time by an X-band ESEEM spectroscopy study of  $^{15}\text{N}$ -substituted superoxide dismutase (SOD). They show a significant difference between two groups of ligands with different orientation relative to the metal ion. The ESEEM spectra of  $^{15}\text{N}$  SOD with cyanide as an inhibitor containing  $^{14}\text{N}$  and  $^{15}\text{N}$  are also discussed. They allow some conclusions to be drawn about structural changes upon inhibitor binding and indicate the necessity of further multifrequency investigations.

**Key words:** Superoxide dismutase (SOD); Electron spin echo envelope modulation (ESEEM) spectroscopy; Histidine residue; Remote nitrogen; Hyperfine coupling

### 1. Introduction

Superoxide dismutase (SOD) is a dimeric metallo-protein containing one  $\text{Zn}^{2+}$  and one  $\text{Cu}^{2+}$  ion per subunit which dismutates the superoxide anion  $\text{O}_2^-$  into  $\text{O}_2$  and  $\text{H}_2\text{O}_2$  [1]. X-ray crystallographic analysis has shown that each copper ion is coordinated to four histidine residues (His-44, His-46, His-61, His-118 following the numbering of the bovine isoenzyme) of which one forms an imidazolate bridge to the  $\text{Zn}^{2+}$  ion [2]. Interaction of SOD with inhibitor molecules such as  $\text{CN}^-$  and  $\text{N}_3^-$  brings about structural changes in the copper coordination without changing the paramagnetism. Thus, electronic magnetic resonance investigations of native SOD and of its complexes with inhibitors are possible and have been performed extensively [3–7]. Also, a number of model complex studies, e.g. on Cu-(imidazole) and related molecules, exist [8–10]. However, an understanding of imidazole ring ligation by probing the hyperfine parameters of the coordinated and the remote nitrogens in native SOD, as well as the effect of inhibitor binding on them, has neither been fully disclosed nor related to structural changes of the copper site. Some information has been obtained from the analysis, by electron paramagnetic resonance (EPR) spectroscopy, of the hyperfine couplings with the directly coordinated nitrogens

which amount to about 40 MHz [3–6]. The remote nitrogen, however, has a significantly smaller interaction. It is inaccessible to EPR and difficult to analyse in electron nuclear double resonance (ENDOR) spectroscopy. So far, only one ENDOR study from cyanide-bound SOD has dealt with the remote nitrogen [7].

On the other hand, the remote  $^{14}\text{N}$  nitrogens from ligated histidine residues of copper proteins show very well pronounced narrow lines in x-band electron spin echo envelope modulation (ESEEM) spectra [11,12]. ESEEM spectroscopy has already been applied to investigate native and inhibitor-bound SOD [13]. The spectra demonstrate a large number of lines from  $^{14}\text{N}$  remote nitrogens in the frequency region 0–5 MHz which are sensitive to pH, removal or substitution of the  $\text{Zn}^{2+}$  ion and to inhibitor binding. However, due to the complex character of ESEEM spectra from four  $^{14}\text{N}$  remote nitrogens, only a qualitative analysis was performed in that work. The complexity may arise, among other reasons, from the different orientations of the imidazole planes in the histidine residues relative to the complex axes as indicated by the crystallographic data [2], which would lead to different hyperfine couplings. In addition, quadrupole interaction of the  $^{14}\text{N}$  nuclei complicates spectra analysis even when its value does not depend on the rotation of the molecular plane. A more preferable situation applies for the use of  $^{15}\text{N}$  which has no quadrupolar interaction (nuclear spin  $I = 1/2$ ). In this work we report the investigation of hyperfine couplings with remote nitrogens in  $^{15}\text{N}$ -substituted native ( $^{15}\text{N}$  SOD) and of  $\text{C}^{15}\text{N}^-$ - and  $\text{C}^{14}\text{N}^-$ -bound SOD.

\*Corresponding author. Fax: (49) (6841) 166 227.

## 2. Experimental

$^{15}\text{N}$ -Labelled  $\text{Cu}_2\text{Zn}_2\text{SOD}$  was isolated from a culture of *Escherichia coli* MC1061 in which the human protein was expressed [14]. The bacterium was grown in minimal medium containing  $(^{15}\text{NH}_4)_2\text{SO}_4$  (Isotec) as the nitrogen source. The protein, produced after overnight induction of the above culture with isopropyl  $\beta$ -D-thiogalactopyranoside, is secreted into the periplasm and released by osmotic shock. SOD was purified to ~95% homogeneity by DEAE Sepharose chromatography (Pharmacia CL-6B).

ESEEM experiments were performed using an X-band Bruker ESP 380 pulsed EPR spectrometer with either dielectric or a split-ring low Q cavity for which the variation of microwave frequency had been secured in the range 9.2–9.8 GHz. The length of the  $\pi/2$  pulse was 16 ns. Two-, three- and four-pulse sequences were used. A four-step phase cycle,  $+(0,0,0)$ ,  $-(0,\pi,0)$ ,  $-(\pi,0,0)$ ,  $+(\pi,\pi,0)$ , in a three  $\pi/2$ -pulse sequence [15] and a cycle,  $+(0,0,0,0)$ ,  $-(0,0,0,\pi)$ ,  $+(0,0,\pi,0)$ ,  $-(0,0,\pi,\pi)$ , in a four-pulse sequence [16] were applied to eliminate unwanted features from experimental echo envelopes. In a one-dimensional version of a four-pulse HSCORE experiment  $\pi/2-\tau-\pi/2-t_1-\pi-t_2-\pi/2-\tau$ -echo [17], a refocusing  $\pi$  pulse, was applied at time  $T/2$  after the second pulse so that  $t_1 = t_2 = T/2$  and the echo amplitude was recorded as a function of time  $T$  which was increased in a step-wise manner. The experiments were performed at 4–5 K using an Oxford CF 935 cryostat.

Cosine and modulus Fourier-transformed ESEEM spectra were obtained without restoration into the dead-time region after fitting of relaxation decays by polynomials of various degrees, normalizing the modulating to the relaxation decay and subtracting the average value [12]. Dead-times were equal to  $\tau = 120$  ns for two-pulse envelopes and to  $(\tau + 24)$  ns for three- and four-pulse spectra. The increment steps for  $\tau$  in the two-pulse experiments were 8 and 16 ns for  $T$  in three- and four-pulse data. Spectra simulations were performed taking into account these dead-times.

## 3. Results and discussion

### 3.1. Native SOD

For the study of SOD samples two-, three- and four-pulse ESE sequences have been used. The three-pulse ESEEM from an  $I = 1/2$  nucleus contains the frequencies of basic nuclear transitions,  $\nu_\alpha$  and  $\nu_\beta$ , each of which corresponds to one of the two states of the electron spin. The two- and four-pulse sequences additionally produce two combination modulation frequencies,  $\nu_\alpha \pm \nu_\beta$  [11,12,16]. In completely or partially orientationally disordered systems not all of these transitions give well-pronounced lines in ESEEM spectra due to the orientational dependence of frequency positions and intensities. Fig. 1 depicts the three-pulse ESEEM spectra obtained for  $^{15}\text{N}$  SOD upon excitation at different magnetic field positions of the EPR spectrum at  $\tau = 312$  ns with a microwave frequency of 9.3485 GHz. Almost all of them reveal the presence of four lines in the frequency region 0–3 MHz, marked at different field positions. The best conditions for the appearance of the two central lines,  $\nu_{\alpha 2}$ ,  $\nu_{\beta 2}$ , with maxima at 1.1–1.2 MHz and 1.8–1.9 MHz, respectively, exist, however, only in the time interval 300–350 ns. The most intensive line  $\nu_{\alpha 1}$ , at low frequencies (0.3–0.4 MHz) exists at values of  $\tau$  between 150 and 600 ns. In contrast, the line  $\nu_{\beta 1}$ , with the higher frequency, 2.6–2.8 MHz, develops its maximum intensity at  $\tau$  values of 500–600 ns. The very sharp line at about 1.4 MHz marked (\*) in the spectrum taken at 3,300 G corre-

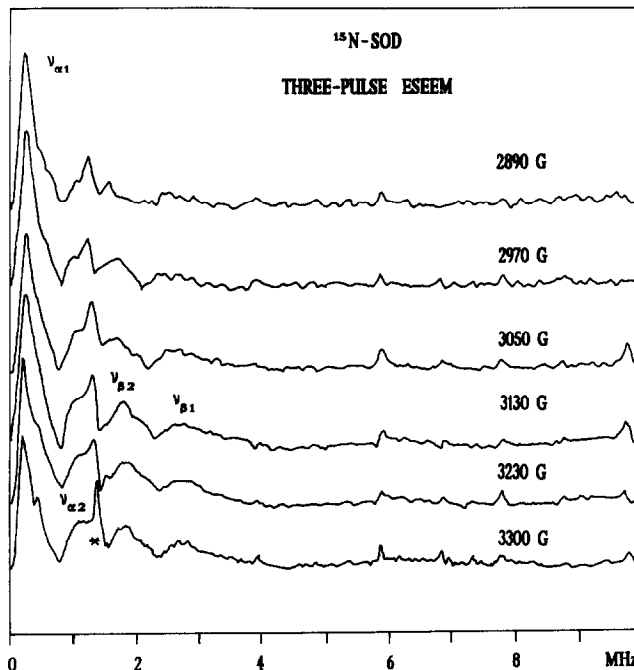


Fig. 1. Three-pulse ESEEM spectra ( $\tau = 312$  ns) of  $^{15}\text{N}$  SOD obtained at different parts of the EPR spectrum using a microwave frequency of 9.348 GHz.

sponds to the matrix nuclear Zeeman frequency of  $^{15}\text{N}$ ; the corresponding lines of other fields are present in the other spectra also.

Fig. 2 shows the three-pulse ESEEM spectrum obtained at  $\tau = 592$  ns for SOD (top) and for  $\text{Cu}^{2+}$ - $(^{15}\text{N}$  imidazole) $_4$  (bottom) recorded under comparable conditions at the high-field edge of the EPR spectrum. A comparison of these spectra indicates that the position of the right outer line,  $\nu_{\beta 1}$ , in SOD corresponds to the position of the respective line in the spectrum of  $\text{Cu}^{2+}$ -imidazole) $_4$ . This correspondence is also confirmed in other fields and in two- and four-pulse spectra (data not shown). Therefore, part of the remote nitrogen nuclei in SOD has hyperfine parameters identical or very close to those in the  $\text{Cu}^{2+}$ - $(^{15}\text{N}$  imidazole) $_4$  complex. Crystallographic data [18], ENDOR investigations in frozen solution [8,9] and, most recently, orientationally selected ESEEM studies of this complex [19], indicate that the planes of imidazole ligands are perpendicular to the complex axis, i.e. parallel to the direction of maximal principal value of  $g$ -tensor. The planes of His-46 and His-44 in SOD align, with good accuracy, also with that direction [2]. Therefore we suggest that the remote nitrogens of His-46 and His-44 possess hyperfine coupling similar to the coupling of remote nitrogens in the model complex. This conclusion is supported by the ESEEM spectra of the  $^{14}\text{N}$  remote nitrogens in SOD and  $\text{Cu}^{2+}$ -imidazole) $_4$  reported by Fee et al. [13] since the three-pulse spectra of both systems contain the line of double-quantum transition of remote nitrogens at 4 MHz. The posi-

tion of this line is determined mainly by the isotropic hyperfine coupling.

By the same consideration, the remote nitrogens of two other histidine residues, His-61 and His-118, which have their imidazole plane tilted with respect to the other histidines and aligned more closely with the complex plane, create the new lines,  $\nu_{\alpha 2}$  and  $\nu_{\beta 2}$ , in the middle part of the ESEEM spectra. The resolution of the spectra, however, is insufficient to reveal differences in the hyperfine constants within each group of nitrogens. Therefore, we shall discuss the spectra as being formed by two groups of ligand remote nitrogens corresponding to two groups of imidazole plane orientations.

Because the new line in SOD is located closer to the position of  $^{15}\text{N}$  Zeeman frequency, the nitrogens of these molecules have a smaller hyperfine coupling with a value of  $\sim 1$ – $1.5$  MHz. Also the three-pulse spectra of Fig. 1 show that the variation of excitation point has no strong influence on the line positions. Therefore, the isotropic hyperfine coupling mainly determines the line positions of both groups of nuclei. Further information useful for the determination of the hyperfine couplings can be obtained from the position of the combination harmonics which appear in the two- and four-pulse ESEEM spectra. However, the two-pulse envelopes of native SOD have a relatively fast relaxation decay which leads to an increase of the line widths, a decrease of line intensities of basic transitions, and to overlap of the line of the basic transition located close to the double Zeeman frequency with that of the sum combination harmonics slightly shifted from that frequency to the higher side (data not shown). Four-pulse spectra avoid these disadvantages due to their significantly slower relaxation decay. Fig. 3

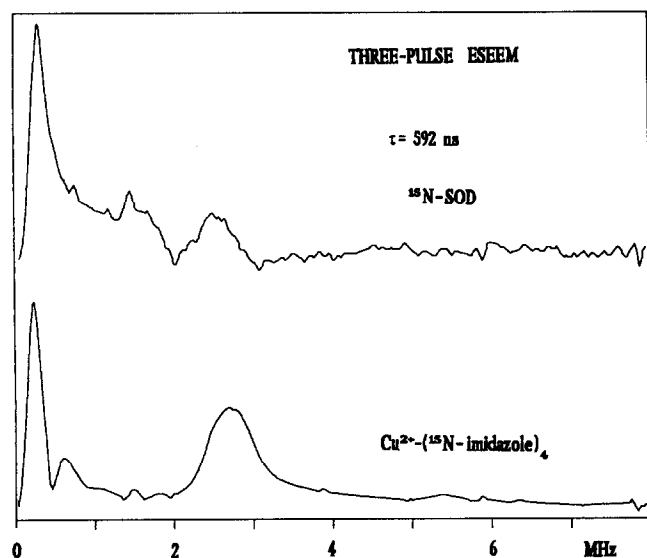


Fig. 2. Comparison of three-pulse ESEEM spectrum of  $^{15}\text{N}$  SOD obtained at  $\tau = 592$  ns and at a magnetic field of 3,235 G (microwave frequency 9.364 GHz) with the spectrum of the model complex  $\text{Cu}^{2+}$ -( $^{15}\text{N}$  imidazole) $_4$  obtained under comparable conditions.

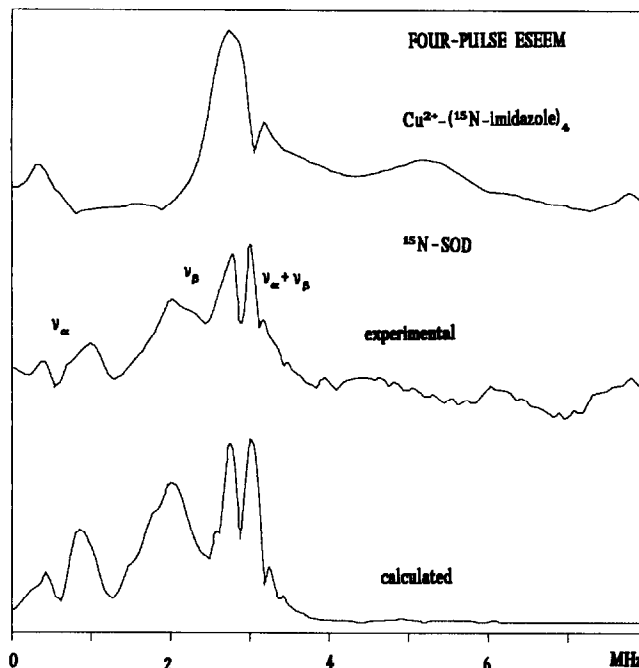


Fig. 3. Four-pulse ESEEM spectra ( $\tau = 344$  ns) of  $\text{Cu}^{2+}$ -( $^{15}\text{N}$  imidazole) $_4$  and of  $^{15}\text{N}$  SOD obtained at 3,395 G (microwave frequency 9.819 GHz). A comparison of the last spectrum with a calculated one for parameters of remote nitrogens is given in the text.

(top recording) shows the four-pulse ESEEM spectrum of  $\text{Cu}^{2+}$ -( $^{15}\text{N}$  imidazole) $_4$  obtained with a microwave frequency of 9.819 GHz in the field of 3395 G corresponding to the maximum of the EPR spectrum and using  $\tau = 344$  ns. It shows the existence of two lines located around 3 MHz. The line with the larger intensity at 2.75 MHz corresponds to one of the nuclear basic transitions of the remote nitrogens because it is also present in the three-pulse spectrum (cf. Fig. 2, bottom). The line with the smaller intensity at 3.18 MHz appears only in four-pulse spectra and thus is related to the sum combination harmonic,  $\nu_{\alpha} + \nu_{\beta}$ . Fig. 3 (middle) also gives the four-pulse spectrum of native SOD obtained under comparable conditions. It clearly indicates the existence of new lines of the basic transitions located at the same frequencies as discussed above in the three-pulse spectra. However, in addition, a new intensive line with a maximum at 3.0 MHz is observed which can be attributed to the sum combination line from the remote nitrogens of histidines His-61 and His-118, which have their imidazole planes rotated. Usually, when intensive sum combination harmonic lines are observed in orientationally disordered ESEEM spectra, their maxima correspond to the turning point of the  $\nu_{\alpha} + \nu_{\beta}$  lineform. The analytical expression for the maximum position is given by the formula [20]:

$$(\nu_{\alpha} + \nu_{\beta})_{\max} = 2\nu_I \left\{ 1 + \frac{\frac{9}{16} T_{\perp}^2}{\nu_I^2 - (T_{\perp} + 2a)^2/16} \right\}^{1/2} \quad (1)$$

A recent analysis of the position of the maxima of sum combination harmonics in orientationally selected ESEEM spectra from  $\text{Cu}^{2+}$ - $(^{15}\text{N imidazole})_4$  has shown good correspondence of experimental maxima and theoretically predicted positions, especially in the  $g_{\perp}$  region where the broad set of complex orientations is excited [19]. Assuming that these conditions are also valid for SOD we can use Eq. 1 to estimate the anisotropic part of the hyperfine interaction with the remote nitrogens in His-61 and His-118. A consideration of the line positions in three-pulse ESEEM spectra yields an isotropic coupling  $a \sim 1$ – $1.5$  MHz which is small compared with the model complex but still significantly exceeds the anisotropic contribution. Under these conditions the second term in the denominator,  $v_I^2 - (T_{\perp} + 2a)^2/16$  plays a negligible role and an approximate expression is valid [20],

$$(v_{\alpha} + v_{\beta})_{\max} = 2v_I + \frac{9}{16} \cdot \frac{T_{\perp}^2}{v_I} \quad (2)$$

which allows the direct estimation of the principal values of the anisotropic hyperfine tensor ( $-T_{\perp}$ ,  $-T_{\perp}$ ,  $2T_{\perp}$ ) in the approximation of axially symmetrical hfi from the shift of the maximum of the sum combination harmonic toward higher frequencies beyond the  $^{15}\text{N}$  double Zeeman frequency. From Fig. 3 the shift of the sum combination harmonic (3.0 MHz) relative to  $2v_I = 2.93$  MHz amounts to 0.07 MHz which yields  $|T_{\perp}| = 0.42$  MHz. Similar values of  $|T_{\perp}|$  have been obtained from ESEEM spectra of native SOD obtained under other conditions. Thus we estimate  $|T_{\perp}|$  with remote nitrogens in His-61 and His-118 to be of the order of 0.4–0.45 MHz.

Adopting now the values recently found for the remote nitrogens in  $\text{Cu}^{2+}$ - $(^{15}\text{N imidazole})_4$  ( $a = 2.4$  MHz,  $T_{\perp} = -0.39$  MHz, and the angle between the directions of maximal principal values of the axial  $g$  and hyperfine tensors  $\vartheta_{\parallel} = 40^{\circ}$ ) [19] for the corresponding nitrogens of His-46 and His-44, we achieved good agreement between simulated and experimental four-pulse ESEEM spectra, including basic as well as sum combination frequencies (Fig. 3, bottom) at values of  $a = 1.1$  MHz,  $T_{\perp} = -0.43$  MHz ( $\pm 0.03$  MHz) and  $\vartheta_{\parallel} \sim 20$ – $30^{\circ}$  for the remote nitrogens of His-61 and His-118. Since the experimental spectrum was taken at the point of maximal intensity in the ' $g_{\perp}$ ' region, the simulations were performed by averaging the projection of  $H_0$  on the complex perpendicular to the complex symmetry and including deviations from this plane up to  $10^{\circ}$ .

The value for the smaller hyperfine coupling also explains the new line appearing around 3 MHz reported by Fee et al. in ESEEM spectra of  $^{14}\text{N}$ -containing SOD in comparison with the model complex (cf. Fig. 1 of [13]), which was also observed in our three-pulse spectra of  $^{14}\text{N}$  SOD. Preliminary simulations with quadrupole parameters typical for remote nitrogen in copper complexes together with hyperfine couplings corresponding to the

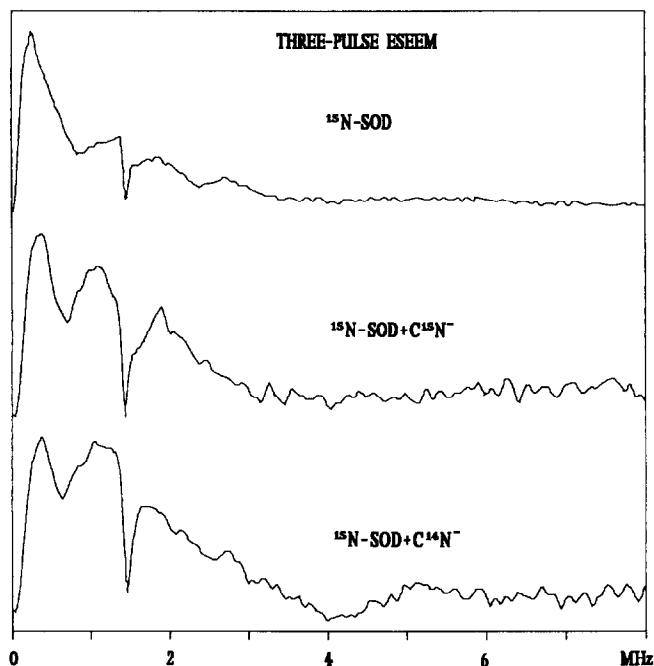


Fig. 4. Three-pulse ESEEM spectra ( $\tau = 312$  ns) of native  $^{15}\text{N}$  SOD, and of SOD bound with inhibitors ( $\text{C}^{15}\text{N}^-$  and  $\text{C}^{14}\text{N}^-$ , respectively). The corresponding envelopes were obtained at 3,300 G using a microwave frequency of 9.753 GHz.

values derived above but translated to  $^{14}\text{N}$ , indicate that the new line is due to a double quantum transition.

### 3.2. Inhibitor ( $\text{CN}^-$ )-bound SOD

Fig. 4 shows the comparison of three-pulse ESEEM spectra of native SOD and SOD bound with  $\text{C}^{14}\text{N}$  and  $\text{C}^{15}\text{N}$  inhibitors. Binding of  $\text{C}^{15}\text{N}$  has some influence on ESEEM spectra which still contain two central lines flanking the  $^{15}\text{N}$  Zeeman frequency line as well as the low frequency component. However, the line close to 3 MHz disappeared and the intensity of the low frequency component is smaller. There do not seem to be new lines of significant intensity from the cyanide nitrogen. The presence of  $\text{C}^{14}\text{N}$  only slightly changes the part of spectra below the  $^{15}\text{N}$  Zeeman frequency, e.g. via a decrease in the intensity of the lowest component. In the region of higher frequencies only one broad asymmetrical peak is detected, ranging up to approximately 4 MHz. A slight increase in intensity between 4 and 6 MHz is also observed. The three-pulse spectra thus demonstrate some influence of the  $\text{C}^{14}\text{N}$  inhibitor but do not yield pronounced and separated lines sufficient for analysis.

From the changes involving the line at about 3 MHz in the three-pulse spectra one can conclude that the inhibitor substitutes one of the histidines with the larger hyperfine constant of the remote nitrogens (i.e. His-44 or His-46) because the outer lines from these nuclei lose intensity and the central part of the spectra where nitrogens of His-61 and His-118 contribute changes only

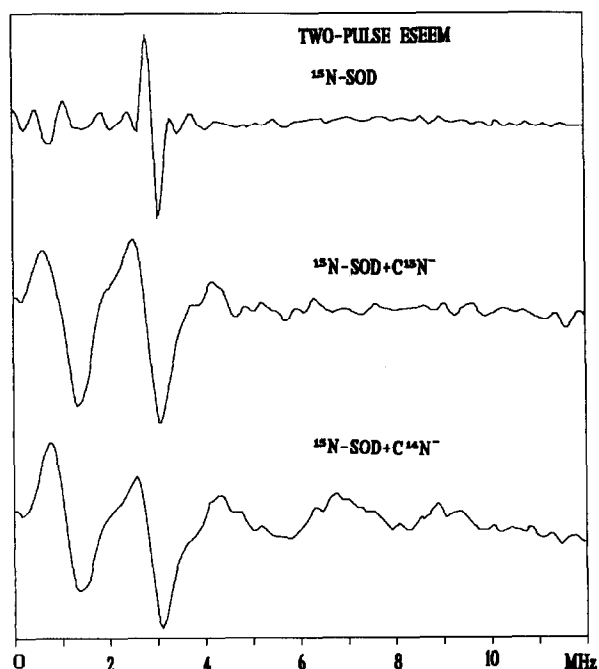


Fig. 5. Cosine Fourier-transformed ESEEM spectra of native  $^{15}\text{N}$  SOD, and of SOD bound with inhibitors ( $\text{C}^{15}\text{N}^-$  and  $\text{C}^{14}\text{N}^-$ , respectively). The corresponding envelopes were obtained under similar conditions at magnetic fields of 3,400–3,410 G using microwave frequencies in the range 9.75–9.77 GHz. The large shape of the lines in the two bottom spectra are connected with a significantly shorter relaxation decay of two-pulse envelopes than for the top spectrum.

slightly. However, the line of higher basic harmonic located close to the intensive sum combination harmonic as in Fig. 3 still clearly develops in four-pulse ESEEM spectra of inhibitor-bound  $^{15}\text{N}$  SOD (data not shown). Therefore the hyperfine interaction with the remaining nitrogen of this group does not change significantly.

Stronger spectral changes are observed in two-pulse ESEEM, as shown in Fig. 5. The cosine Fourier-transformed two-pulse ESEEM spectrum of  $^{15}\text{N}$  SOD bound with  $\text{C}^{15}\text{N}^-$  clearly demonstrates the appearance of a new intense line with negative amplitude compared with the native sample. The spectrum of the  $\text{C}^{14}\text{N}^-$ -bound SOD also contains such a line of the negative amplitude in this frequency region and an additional broad peak around 7 MHz. This line changes its position (by  $\sim 0.5$  MHz) and intensity ( $\sim$  two times between limiting cases) in the two-pulse spectra obtained at the different points of the EPR spectra with both inhibitors. A detailed comparison of its orientational dependence in the two cases indicates a different behaviour, implying that these lines are due to the cyanide nitrogen. In the  $^{15}\text{N}$  spectrum it can be related to the difference combination harmonic [11,12]; for  $^{14}\text{N}$  it is more difficult to relate this line so definitively. Van Camp et al. [7], after analysis and simulations of ENDOR spectra of  $^{14}\text{N}$  SOD with cyanide inhibitors containing both nitrogen isotopes, gave values of 5.5–8.0

MHz for the hyperfine coupling with cyanide  $^{15}\text{N}$  depending on the magnetic field orientation relative to  $g$ -tensor axes. The remote histidine nitrogens were taken into account in their simulations as three equivalent nuclei with a coupling translating to 2.26 MHz for  $^{15}\text{N}$ . Our data indicate, however, that the main contribution in the spectra of remote nitrogens comes from two nitrogens (His-61 and His-118) with about two-times smaller coupling. The value reported for the cyanide nitrogen coupling [7] is close to the border of hyperfine interactions at which the  $^{15}\text{N}$  nucleus does not give noticeable modulation amplitudes in the X-band [21,22]. The absence of new lines of significant amplitude in three-pulse ESEEM spectra of  $\text{C}^{15}\text{N}^-$ -SOD confirms, therefore, the order of the value given by van Camp et al. [7]. Our data are, however, not sufficient for quantitative analysis of the cyanide nitrogen interaction. Further investigations of this system should be connected with multifrequency ESEEM experiments. Measurements at lower and higher microwave frequencies should be performed in order to find conditions for narrow, intense lines from the histidines which allow for differentiation of the coupling differences between the nitrogens of each group and also from cyanide nitrogen.

The finding that the histidine residues 44 and 46 are involved in the structural changes upon cyanide binding to SOD is in agreement with NMR data which indicate that, upon cyanide binding, His-46 is detached and  $\text{CN}^-$  binds to copper. Together with the other three histidines,  $\text{CN}^-$  produces a square planar configuration [23].

*Acknowledgements:* S.D. acknowledges the receipt of an Alexander von Humboldt Foundation Research Fellow Award and the hospitality of the Biophysics Department of Saarland University. A.S. thanks the Deutsche Forschungsgemeinschaft for a grant supporting his stay at Saarland University, and the Biophysics Department for its hospitality. I.F. gratefully acknowledges support from Progetto Vigoni during her stay at the Biophysics Department. The authors thank Dr. R. Kappl and Mr. H. Reinhard for their help in the preparation of inhibitor bound samples. Thanks are expressed to Dr. G. Mullenbach and to Chiron Corporation (Emeryville, CA, USA) for allowing M.S.V. to prepare  $^{15}\text{N}$ -labelled SOD.

## References

- [1] McCord, J.M. and Fridovich, I. (1969) *J. Biol. Chem.* 244, 6049–6055.
- [2] Tainer, J.A., Getzoff, E.D., Beem, K.M., Richardson, J.S. and Richardson, D.C. (1982) *J. Mol. Biol.* 160, 181–217.
- [3] Lieberman, R.A., Sands, R.H. and Fee, J.A. (1982) *J. Biol. Chem.* 257, 336–344.
- [4] Rotilio, G., Morpurgo, L., Giovagnoli, C., Calabrese, L. and Mondovi, B. (1972) *Biochemistry* 11, 2187–2192.
- [5] Hüttermann, J., Kappl, R., Banci, L. and Bertini, I. (1988) *Biochim. Biophys. Acta* 956, 173–188.
- [6] Hüttermann, J. (1993) in: *Biological Magnetic Resonance* Vol. 13 (Berliner, L.J. and Reuben, J., eds.) pp. 219–252, Plenum, New York.
- [7] Van Camp, H., Sands, R.H. and Fee, J.A. (1982) *Biochim. Biophys. Acta* 704, 75–89.

- [8] Scholl, H.-J. and Hüttermann, J. (1992) *J. Phys. Chem.* 96, 9684–9691.
- [9] Van Camp, H.L., Sands, R.H. and Fee, J.A. (1981) *J. Chem. Phys.* 75, 2098–3008.
- [10] Mims, W.B. and Peisach, J. (1978) *J. Chem. Phys.* 69, 4921–4932.
- [11] Mims, W.B. and Peisach, J. (1989) in: *Advanced EPR. Applications in Biology and Biochemistry* (Hoff, A.J., ed.) pp. 1–57, Elsevier, Amsterdam (and references therein).
- [12] Dikanov, S.A. and Tsvetkov, Yu.D. (1992) *Electron Spin Echo Envelope Modulation (ESEEM) Spectroscopy*. Ch. 15, CRC Press, Boca Raton (and references therein).
- [13] Fee, J.A., Peisach, J. and Mims, W.B. (1981) *J. Biol. Chem.* 256, 1910–1914.
- [14] Getzoff, E.D., Cabelli, D.E., Fisher, C.L., Parge, H.E., Viezzoli, M.S., Banci, L. and Hallewell, R.A. (1992) *Nature*, 358, 347–351.
- [15] Fauth, J.-M., Schweiger, A., Braunschweiler, L., Forrer, J. and Ernst, R.R. (1986) *J. Magn. Res.* 66, 74–85.
- [16] Gemperle, C., Aebli, G., Schweiger, A. and Ernst, R.R. (1990) *J. Magn. Res.* 88, 241–256.
- [17] Höfer, P., Grupp, A., Nebenführ, H. and Mehring, M. (1986) *Chem. Phys. Lett.* 132, 279–283.
- [18] McFadden, D.L., McPhail, A.T., Garner, C.D. and Mabbs, F.E. (1976) *J. Chem. Soc., Dalton Trans.* 47–52.
- [19] Dikanov, S.A., Spoyalov, A.P. and Hüttermann, J. (1994) *J. Chem. Phys.* (in press).
- [20] Reijerse, E.J. and Dikanov, S.A. (1991) *J. Chem. Phys.* 95, 836–845.
- [21] Magliozzo, R.S. and Peisach, J. (1992) *Biochemistry* 31, 189–199.
- [22] Dikanov, S.A., Burgard, C. and Hüttermann, J. (1993) *Chem. Phys. Lett.* 212, 493–498.
- [23] Banci, L., Bencini, A., Bertini, I., Luchinat, C. and Piccioli, M. (1990) *Inorg. Chem.* 29, 4867–4873.